

A Method in Extracting Vegetation Quality Parameters Using Hyperion Images, with Application to Precision Farming

M.R. Mobasheri, Y. Rezaei and M.J. Valadan Zoej

Department of Remote Sensing, KNToosi University of Technology,
Mirdamad Cross, Valiasr Ave. P.O. Box 15875-4416, Post Code 1996715433, Tehran, Iran

Abstract: High spectral resolution in hyperspectral images and their ability of imaging in narrow bands, make them highly capable in investigating and monitoring vegetation and crops. Due to the high number of bands in the hyperspectral images, selection of optimum bands for monitoring a specific parameter is necessary. For this, absorption bands of different crop surface materials and the relevant predefined indices can be deployed. In this research, regarding the absorption bands of the substances under consideration, 17 optimum bands were selected. Then, using these bands, different vegetation indices are introduced and calculated using supplied Hyperion images. The result of applying each index on the image was investigated and the outcoming results were classified into different regions. To access to the applicable results, Decision Tree Classification method was used in the second stage. The output results of this method of classification showed that it can be deployed for the detection of the canopy water stress and as a whole, the health of the vegetation under study in the region. Also this research showed that by using these images, one can investigate and monitor the green vegetation and the parameters affecting their health as well as discovering their stresses in which often cannot be detected by eyes, otherwise.

Key word: Hyperspectral imaging • absorption bands • vegetation indices • decision tree classification • precision farming

INTRODUCTION

Remote sensing technology is being increasingly used for the measurement of necessary parameters in the cropland monitoring for the purpose of precision farming and in forestry. By deployment of broadband sensors, large amount of information from the earth's surface has been collected which was not accessible otherwise. Through this information one could regularly update map of vegetation cover in large scales. The new technology showed that although the information produced by broadband sensors was useful in many applications but, it had its own limitations. That is, because of the limited number of bands and their relatively wide width, large amount of information about vegetation will be lost during averaging.

Most of the natural features have special spectral signals that occur in a very narrow region of the electromagnetic spectrum. Consequently, for identification and recognition of these signals, narrow band sensors are needed.

Thus, wide band sensors such as MSS and TM on board of Landsat series of satellites would not be able to detect signals in the very narrow bands because of their 100 to 200nm spans as well as their discrete bands. To overcome this problem, a Hyperspectral sensor with a continuous spectrum is a powerful tool and can be used for effective studies in precise reconnaissance of land covers and environmental parameters.

The spectral reflectance of natural surfaces is sensitive to the special chemical junction of the molecules of substances in different states of solid, liquid and gas. Diversity of the elements in a substance compound causes the variety of the shape and location of the absorption bands of that substance in the electromagnetic spectrum. Then the vast diversity of substances in the real world can produce a complicated signal that sometimes is hard to interpret.

Each pixel has its own spectrum that enables us to produce a map of the presence and abundances of the chemical junctions present in the surface of that pixel. By analysis of the spectral features and recognition of those

chemical junctions, one could determine the location of the occurrence from which the map of distribution would be producible. This kind of spectrometry has different names among which we can name Imaging Spectrometry, Hyperspectral Remote Sensing and Hyperspectral Imaging. One of the areas that have the most application in Hyperspectral Remote Sensing is vegetation canopies. The increase in the precision of the determination of the plant species, plant health and the amount of stresses in the plants (such as water, fertilizers, etc), renders precision farming possible. The extraction of these kinds of information from Hyperspectral Remote Sensing imageries is the object of this work.

Fundamental factors affecting vegetation reflectance:

Downward sun radiant energy is the most important source of energy for numerous biological processes in vegetation. The interaction between sun irradiance and vegetations can be divided in to three groups: thermal effects, Photosynthesis and Photogeomorphogenic effects. More than 70% of the absorbed energy by vegetation converts to heat where it consumes for the evapotranspiration and thermal equilibrium [1-3].

The Photosynthetically Active Radiation (PAR) that constitute 28% of the absorbed radiation, will be used for synthesis and conversion to energetic organic compounds. The light characteristics of the leaves in the PAR region depends on the radiation conditions, leaf thickness, leaf surface structures, the amount of leaf chlorophyll and carotenoids, the amount of leaf dry substance in unit area and leaf internal structure [4].

A beam of sun irradiance falling on a leaf surface undergoes reflection, transmission and or absorption. The amount of reflected, transmitted and absorbed energy depends on wavelength, incidence angle, surface smoothness and roughness, spectral characteristics of the bio-chemical contents of the leaves [5, 6]. The first contact of the beam is with leaf surface which is made of cuticle and epidermal layers where in some leaves these layers might be covered by wax that may alter the amount of reflected, transmitted and absorbed energy. On the other hand the amount of light which is absorbed by or transmitted through the leaf depends on the pigments selectivity.

The visible portion of the leaf reflectance spectrum is characterized by high absorption of pigments. For instance the chlorophyll pigments absorb violet, blue and red but green, so most of vegetation has green appearance. The reflectance spectrum of green vegetation has maximum absorption at 420, 490 and 660 nanometers bands all by chlorophyll. The principal and important

Table 1: Principal pigments of vegetation and their wavelengths of maximum absorption

Pigment	Wavelength of maximum absorption
Chlorophyll a	420, 490, 660
Chlorophyll a	435, 643
β Carotene	425, 450, 480
α Carotene	420, 440, 470
Xanthophyll	425, 450, 475

pigments and their maximum absorption wavelengths are shown in Table 1.

The electromagnetic absorption mechanism in the pigments of green vegetation is by atomic excitation [7, 8]. Pigments such as chlorophyll and carotenes, absorb light in particular wavelength, causing an electron jump in the pigment molecular structures. The energy produced by de-excitation, will be consumed for electro-chemical reactions [9].

In the period of senescence, faster degradation of chlorophylls compare to carotenes [4] causes significant increase in the red wavelength due to the great decrease in the chlorophyll pigment density. In this case carotenes and Xanthophylls are majority in the leaf where they absorb blue and reflect green and red hence leaves will have yellow appearance. By death of brown pigments (tannins) leaf reflectance and transmittance in 400-700 nanometers decrease [4].

MATERIALS AND METHODS

Region of study: The image used for this work was a Hyperion image of May21, 2002 from a region in the south of Tehran capital of I. R. of Iran (Fig. 2). Hyperion is a Hyperspectral sensor on board of EO-1. It has 224 band in the 400 to 2500nm spectral region. Its spatial resolution is 30m with a swath width of 7.5km.

Preprocessing and atmospheric correction: For removing the effects of atmosphere from the image, algorithms such as ACORN, ATCOR or FLAASH can be used. In this work we used FLAASH software based on MODTRAN algorithm in ENVI. To do this we first should convert DN to physical quantities such as radiance.

The Hyperion image in hand was in Level 1 on which only the radiometric corrections were done. Also only 196 bands out 224 were calibrated. These bands were 8 to 57 in the visible and near infrared (VNIR) and 77 to 224 for shortwave IR (SWIR). One of the problems in Hyperion images was that the sensors VNIR and SWIR have one pixel misplacing after detector 128 in the CCD array. This misplacing was corrected at this stage resulted in

Table 2: List of indices used in this research, ρ is reflectance

Index application	Index name	Index equation	Reference No.
Indices showing vegetation cover	Red edge normalized difference vegetation index	$NDVI_{705} = \frac{\rho_{750} - \rho_{705}}{\rho_{750} + \rho_{705}}$	[8, 13]
	Modified red edge normalized difference vegetation index	$mNDVI_{705} = \frac{\rho_{750} - \rho_{705}}{\rho_{750} + \rho_{705} - 2\rho_{445}}$	[8, 14]
Index showing nitrogen content	Normalized difference nitrogen index	$NDNI = \frac{\log(1/\rho_{1510}) - \log(1/\rho_{1680})}{\log(1/\rho_{1510}) + \log(1/\rho_{1680})}$	[1, 2]
Index showing dry or senescent	Cellulose absorption index	$CAI = 0.5 \left(\frac{\rho_{2000} - \rho_{2200}}{\rho_{2100}} \right)$	[15, 16]
leaves carbon content	Plant senescence reflectance index	$PSRI = \frac{\rho_{680} - \rho_{500}}{\rho_{750}}$	[11]
Index showing leaf pigments	Carotenoid reflectance index 1	$CRI1 = \left(\frac{1}{\rho_{510}} \right) - \left(\frac{1}{\rho_{550}} \right)$	[17]
	Carotenoid reflectance index 2	$CRI2 = \left(\frac{1}{\rho_{510}} \right) - \left(\frac{1}{\rho_{700}} \right)$	[17]
	Anthocyanin reflectance index 1	$ARI1 = \left(\frac{1}{\rho_{530}} \right) - \left(\frac{1}{\rho_{700}} \right)$	[18]
	Anthocyanin reflectance index 2	$ARI2 = \rho_{800} \left[\left(\frac{1}{\rho_{530}} \right) - \left(\frac{1}{\rho_{700}} \right) \right]$	[18]
Index showing canopy water content	Normalized difference water index	$NDWI = \frac{\rho_{857} - \rho_{1241}}{\rho_{857} + \rho_{1241}}$	[19]
	Moisture stress index	$MSI = \frac{\rho_{1599}}{\rho_{819}}$	[20, 21]
	Normalized difference infrared index	$NDII = \frac{\rho_{819} - \rho_{1649}}{\rho_{819} + \rho_{1649}}$	[22, 23]

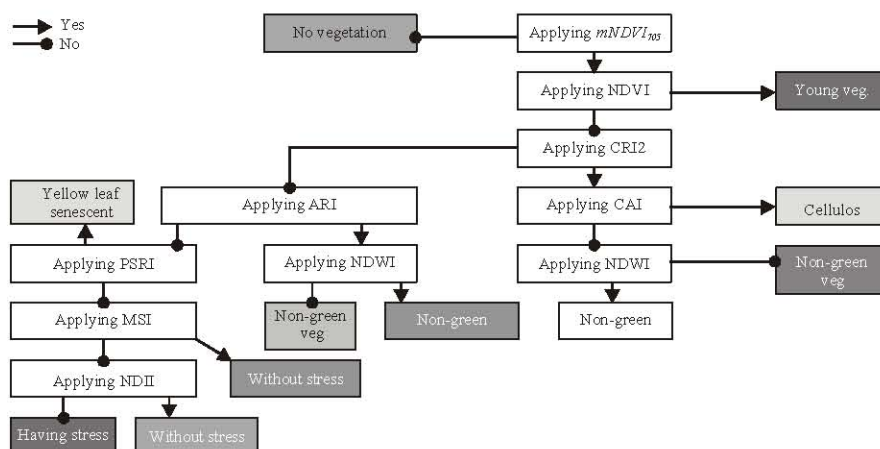


Fig. 1: Schematic diagram of the flowchart showing different stages of classifications

disappearance of the striping effects. Then DN to radiance (L) conversion was done using the following equations:

$$\begin{aligned} L_{VNIR} &= \text{Digital Number}/400 \\ L_{SWIR} &= \text{Digital Number}/800 \end{aligned} \quad (2)$$

In the next stage using FLAASH software and visibility value (from nearest weather station) the correction for the atmospheric effects were carried out. Then using MNF function (Minimum Noise Fraction) those bands with high noises were detected and omitted and so it remained only 157 bands.

Table 3: List of threshold values for the indices used in this work

Index	Application	Threshold and Range	Coverage (%)
<i>mNDVI</i> ₇₀₅	Vegetation cover	0.30-1.0	39.165
NDNI	Plants with high nitrogen content	0.12-1.0	4.999
PSRI	Plants in senescence	0.10-0.25	14.438
CRI	Green vegetation	1.00-11.0	29.343
ARI	Vegetation containing Anthocyanin	0.001-0.1	2.784
NDWI	Green vegetation containing water	0.10-0.4	31.381
MSI	Green vegetation with no water stress	0.00-0.4	15.993
NDNII	Green vegetation regions	0.20-0.6	34.947

After this, to correct for the remaining extra undesired features in the reflectance spectrum and smoothing, the EFFORT function was applied to the image [10, 11]. After corrections for the atmospheric effects and finishing pre-processing, the image will be ready for designing the algorithm.

Methodology in algorithm designing: As is mentioned in the previous section, we can use indices for the detection of features affecting vegetation health based on absorption bands in the vegetation spectrum of each and individual pixels. In the first stage these indices were applied to the images. Then in the next stage a combination of indices were applied to the images, results of which will be discussed later in this section. Table 2 shows a list of indices used in this work. As can be seen these indices have been divided in to 5 groups, indices for detection of vegetation, indices for nitrogen detection, indices showing dry or senescent leaves carbon content, indices showing pigments and indices detecting leaf water content [12].

*NDVI*₇₀₅ is an adopted *NDVI* for use in high spectral resolution images such as Hyperion. The application of this index is in precision farming, forestry and detection of vegetation stresses. This index is sensitive to the small changes in leaf cover, non-vegetated areas and plant senescence. *mNDVI*₇₀₅ index is a modified *NDVI*₇₀₅ corrected for mirror like reflection in vegetation [Datt, B., 1999]. A threshold value of 0.3 for *mNDVI*₇₀₅ is found suitable for this work. This value is achieved through study of ground data and land cover and amount of chlorophyll concentration in selected regions. The result of application of this threshold on the image is shown in Fig. 3 bellow. The threshold for the other indices is also determined and is shown in Table 3.

NDNI is an index for estimation of the relative amount of nitrogen content of vegetation. Those vegetation indices that are sensitive to chlorophyll are usually

sensitive to nitrogen as well [4, 24]. Nitrogen concentration of biomass can affect the reflectance on 1510nm wavelength [4, 24]. The reflectance in this band can be compared with reflectance at 1680nm on which nitrogen concentration does not have any affection. This index varies between 0 and 1 and the range of index in the area specified by *mNDVI*₇₀₅ (Fig. 3) is between 0.01 and 0.12 (Fig. 4 and Table 3).

CAI is the index for the cellulose content of the plant. It absorbs in the 2000 to 2200nm region. This index can be used for senescent plants residue, potential of fire and pasture management. *CAI* generally varies between -3 and 4. This index has not been used directly in our algorithm.

PSRI is an index sensitive to carotenoids such as α and β carotenes. Increase in this index represents increase in the plant stress, beginning of plant senescence and plant fruit ripening. This index varies between -1 and 1 and for the region specified by *mNDVI*₇₀₅ the *PSRI* index varies between 0.1 and 0.25 and the corresponding image is shown in Fig. 5.

CRI is an index sensitive to the carotenoid pigments available in the leaves and stems. Higher values of this index represents higher carotenoid concentration compare with chlorophyll. *CRI2* is a modification of *CRI1* and provides better results in areas of high carotenoid concentration. *CRI2* usually varies between 0 and 15 but in the area specified with *mNDVI*₇₀₅ this index varied between 1 and 11. The image result of this index is shown in Fig. 6.

ARI is the index sensitive to the reflectance by the amount of anthocyanin present in the foliage. An increase in *ARI1* indicates canopy changes in foliage via new growth or death [19]. *ARI2* is a modification of *ARI1* and varies between 0 and more than 0.2. Applying this index on the image for the area specified by *mNDVI*₇₀₅ have resulted in values between 0.001 to 0.1 and is shown in Fig. 7.

NDWI is the index sensitive to the canopy water content [25]. Since the reflectance in 857nm and 1241nm are only differ in the absorption of liquid water, the scattering of 1241nm by the canopy may highlight the canopy water content [26]. Although this index varies between -1 and 1, the range of it in this work and for the region specified by *mNDVI*₇₀₅ was 0.1 to 0.4. The corresponding image is shown in Fig. 8.

MSI is an index sensitive to the increase in the leaf water content by increasing in the absorption in 1599nm wavelength compare to 819nm which is insensitive to the leaf water content and is used as a reference [20, 27]. Higher values of this index shows higher water stresses

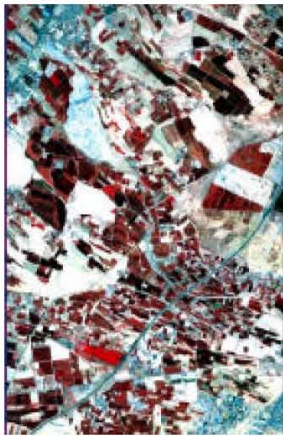


Fig. 2: Image of the region of interest RGB (37, 27, 17)

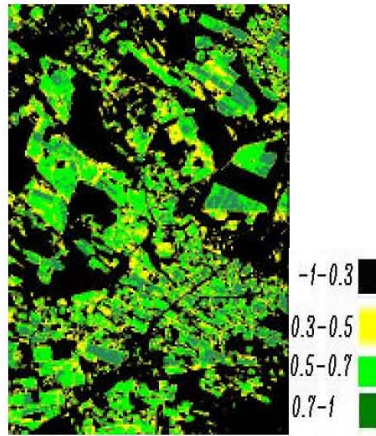


Fig. 3: Image of the region specified by $mNDVI_{705}$ index. This image will be used as a reference image for the rest of the indices

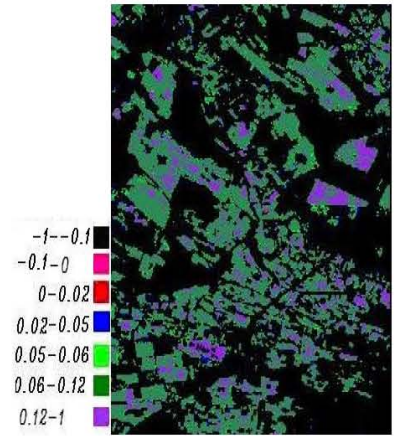


Fig. 4: NDNI index

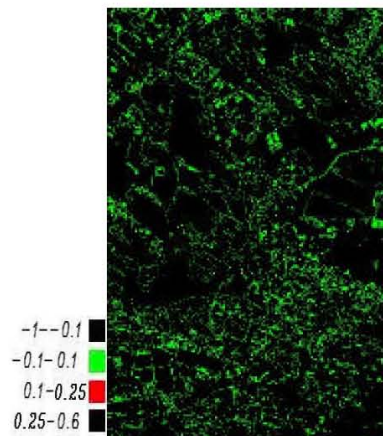


Fig. 5: PSRI index

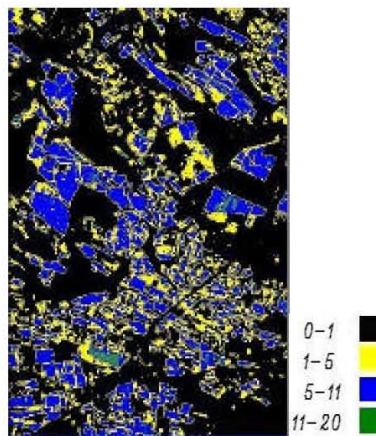


Fig. 6: CRI index

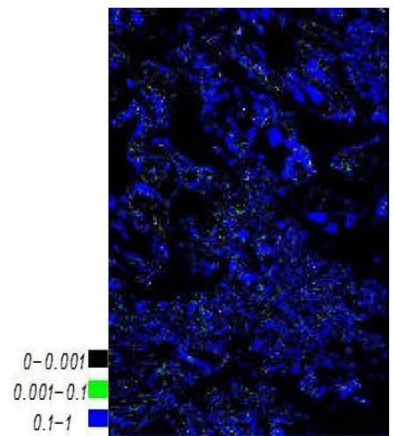


Fig. 7: ARI index

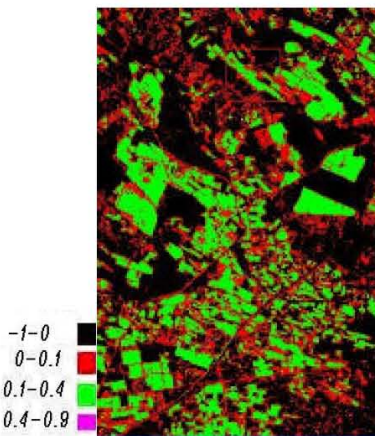


Fig. 8: NDWI index

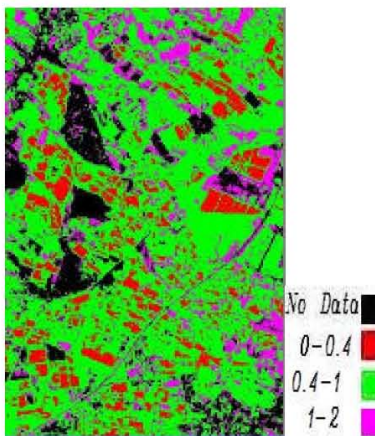


Fig. 9: MSI index

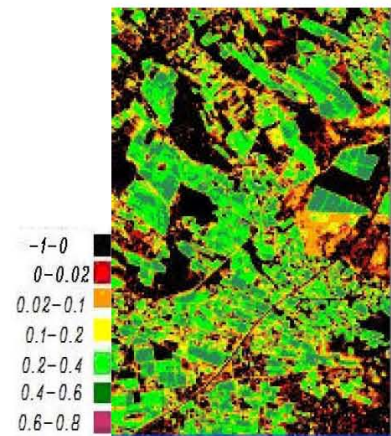


Fig. 10: NDII index

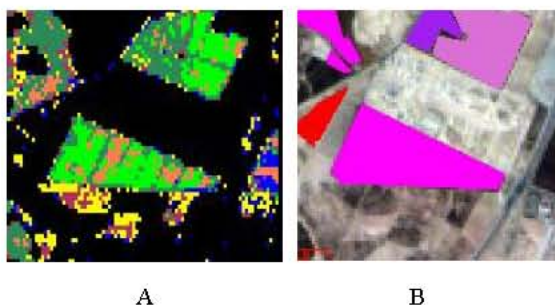


Fig. 11: a) Results of classification in a field showing different health parameters for different parts of the field. b) ground truth showing only one specie in the field

and lower water contents. This index can vary between 0 and 3 but for the area of our interest that is specified by $mNDVI_{705}$, it varied between 0 and 0.4. The resulting image is shown in Fig. 9.

$NDII$ index is also sensitive to the canopy water content and increases proportionally [13, 21]. It varies between -1 and 1 and for our region of interest it varied from 0.02 to 0.6. The output image for this index is shown in Fig. 10.

Figure 2 shows a study area subimage and Fig. 3-10 are the results of the application of the indices to the region specified by $mNDVI_{705}$ image.

As is mentioned, by applying each one of indices on the satellite images, we might be able to monitor the vegetation health. The main problem in the application of these indices is determination of suitable threshold for different applications. This is more problematic at the border of two features hence these kind of pixels contain considerable portion of the image. The other problem is the presence of mixed pixel (mixel) especially at the borders where it renders the correct classification of the image difficult.

Since each one of these indices indicate the characteristics of a particular plant parameter, to access to the precise information, one must analyze these indices simultaneously. To do this, in the second part of our work we applied *Decision Tree Classification* method. This method consists of few stages where we assign a class to each pixel through a binary decision. Namely in each stage through some mathematical conditions, we divide the image in to two classes. Each one of these new classes will undergo another stage and will be divided in to two new classes and so on. Through these stages we may apply every index with its defined threshold and limitations introduced by different sources.

In our work we first applied the red edge index of $mNDVI_{705}$ to separate the vegetated area from non-vegetated. This image is used as a layer image for the rest of indices images. Next by using $NDNI$ the region of high nitrogen content which represents the region with growing vegetation was determined and assigned to class 1. In the 3rd stage carotenoid (CRI), 4th stage cellulose (CAI) for dry and dead vegetation and ARI for the amount foliage, 5th stage, $NDWI$ and $PSRI$ has been applied to separate stressed and the age of the vegetation in to different classes. And finally in the 7th and 8th stage the water content of the vegetation were separated in to different classes by using $NDII$ and MSI indices. Fig. 1 shows a flow chart of the procedures. As a result of these procedures the image was divided in to 11 different classes, one nonvegetated and 10 classes showing different health aspects of the vegetated area. Table 4 summarizes the results of these classifications.

Comparing this Table with Table 3 shows that through application of Decision Tree, some undesired information have been omitted and the classifications have been enhanced.

With refer to Table 4 and with regard to the image acquisition date (harvesting season in the region), one can see that 16% of the vegetated area have ripened (agricultural field ready for harvesting) and 5% of vegetated area is at the growing stage. Also it can be seen that the area which is assigned to unique vegetation species, has been classified into different classes. For instance in Fig. 11 in which the classification results for one field is shown, although the field contains one specie of vegetation but, from health and stresses points of view, different parts of the field has been divided in to different classes. This certainly could not be achieved by multispectral scanner imageries. Using this algorithm we may be able for instance to detect different parts of a vegetated field in which plants are dry and are in the fire risk hazard (yellow region). This is crucial for the forest region. Also the region which is classified as high water content was close to the water channels when we referred to the ground data.

The privilege of using this algorithm for classification is that while using different sources of information, the speed of operation is increased. Moreover, with regard to different applications one can change the indices threshold values and the imposed mathematical conditions at each stage and compare the results with the ground data in order to calibrate the algorithm for a particular condition.

RESULTS AND DISCUSSION

High spectral resolution of hyperspectral images and imaging in narrow bands, provides high ability in assessment and monitoring of vegetation health parameters. Due to the numerous bands in hyperspectral images, selection of optimum band for a particular mandate is compulsory. For this, one may use the position of the absorption bands for the feature under investigation and use the relevant indices. In the case of vegetation growing stage and vegetation health, we must assess different indices simultaneously.

In this work, with regards to the position of absorption bands in the vegetation spectrum, 17 bands were selected in order to construct an algorithm. Using these bands, different indices were introduced and calculated for the image in hand. Then the results of each index was studied and classified in to different regions. To achieve a better result, all these indices were considered simultaneously through Decision Tree Classification method. The output image showed high ability of the method in monitoring and studying the growing and health of vegetated area where it was impossible otherwise. The main problem in using this method was determination of suitable threshold values for each index used. In most cases, we need to carry out some precise field measurements in this regards but once we determined these thresholds, we may use them for the region continuously. Presence of mixed pixels especially in the borders is another problem we faced in this algorithm where it might renders the results uncertain.

REFERENCES

1. Van der Meer F. and Stiven M. de Jong, 2001. Imaging Spectrometry Basic Principals and Prospective Application. Edited by Kluwer Academic Publishers, Dordrecht, ISBN: 1-4020-0194-0.
2. Staenz, K., R.A. Neville, S. Clavette, R. Landry, H.P. White and R. Hitchcock, 2002. Retrieval of surface reflectance from Hyperion radiance data, Geoscience and Remote Sensing Symposium, 2002. IGARSS '02. 2002 IEEE International.
3. Mobasheri, M.R., 2007. Fundamentals of Physics in Remote Sensing and Satellite Technology. Farsi (Ed.). KNTToosi University of Technology Publication, pp: 318.
4. Fourty, T., F. Baret, S. Jacquemoud, G. Schmuck and J. Verdebout, 1996. Leaf Optical Properties with Explicit Description of Its Biochemical Composition: Direct and Inverse Problems. Remote Sensing of Environment 56: 104-117.
5. Curran, P.J., 1989. Remote Sensing of foliar chemistry. Remote Sens. Environ., 30: 271-278.
6. Curran, P.J., J.L. Dungan, B.A. Machler, S.E. Plummer and D.L. Peterson, 1992. Reflectance Spectroscopy of fresh whole leaves for the estimation of chemical concentration. Remote Sens. Environ., 39: 153-166.
7. Belward, A.S., 1991. Spectral characteristics of vegetation, soil and water in the visible, near-infrared and middle- infrared wavelengths. In: Belward, A.A. and C.R. Valenzuela (Eds.). Remote Sensing and Geographical Information Systems for Resource Management in Developing Countries. Kluwer, Netherlands.
8. Verdebout, J., S. Jacquemoud and G. Schmuck, 1994. Optical properties of leaves: Modeling and experimental studies. In: Hill, J. and J. Megier (Ed.). Imaging Spectrometry- A Tool for Environmental.
9. Sims, D.A. and J.A. Gamon, 2002. Relationships Between Leaf Pigment Content and Spectral Reflectance Across a Wide Range of Species, Leaf Structures and Developmental Stages. Remote Sensing of Environ., 81: 337-354.
10. Apan, A., A. Held, S. Phinn and J. Markley, 2004. Detecting sugarcane 'orange rust' disease using EO-1 Hyperion hyperspectral imagery. Intl. J. Rem. Sens., ISSN 0143-1161, vol: 25.
11. Mobasheri, M.R. and Y. Rezaie, 2006. A fast Method for Aerosol Effects Corrections from MODIS Images. Under Review. J. Tech. Res., Tehran University (In Farsi).
12. Elvidge, C.D., 1990. Visible and near infrared reflectance characteristics of dry plant materials. Intl. J. Rem. Sens., 11: 1775-1795.
13. Goodenough, D.G., A. Dyk, K.O. Niemann, J. Pearlman, H. Chen, T. Han, M. Murdoch and C. West, 2003. Processing Hyperion and ALI for Forest Classification. IEEE Transactions on Geoscience and Remote Sensing. 41: 1321-1331.
14. Datt, B., 1999. A New Reflectance Index for Remote Sensing of Chlorophyll Content in Higher Plants: Tests Using Eucalyptus Leaves. J. Plant Physiol., 154: 30-36.
15. Daughtry, C.S.T., 2001. Discriminating Crop Residues from Soil by Short-Wave Infrared Reflectance. Agron. J., 93: 125-131.
16. Daughtry, C.S.T., E.R.Jr. Hunt and J.E. McMurtrey III, 2004. Assessing Crop Residue Cover Using Shortwave Infrared Reflectance. Rem. Sens. Environ., 90: 126-134.

17. Gitelson, A.A., M.N. Merzlyak and O.B. Chivkunova, 2001. Optical Properties and Nondestructive Estimation of Anthocyanin Content in Plant Leaves. *Photochem. Photobiol.*, 71: 38-45.
18. Gitelson, A.A. and M.N. Merzlyak, 1994. Spectral Reflectance Changes Associated with Autumn Senescence of *Aesculus Hippocastanum* L. and *Acer Platanoides* L. Leaves. Spectral Features and Relation to Chlorophyll Estimation. *J. Plant Physiol.*, 143: 286-292.
19. Gitelson, A.A., Y. Zur, O.B. Chivkunova and M.N. Merzlyak, 2002. Assessing Carotenoid Content in Plant Leaves with Reflectance Spectroscopy. *Photochem. Photobiol.*, 75: 272-281.
20. Ceccato, P., S. Flasse, S. Tarantola, S. Jacquemoud and J.M. Gregoire, 2001. Detecting Vegetation Leaf Water Content Using Reflectance in the Optical Domain. *Rem. Sens. Environ.*, 77: 22-33.
21. Hunt, G.R., 1980, Electromagnetic Radiation: The Communications Link in Remote Sensing. In: Siegal, B. and A. Gillespie (Eds.). *Remote Sensing in Geology*, New Yourk, Wiley, pp: 702.
22. Hunt, Jr.E.R. and B.N. Rock, 1989. Detection of Changes in Leaf Water Content Using Near and Middle-Infrared Reflectances. *Rem. Sens. Environ.*, 30: 43-54.
23. Merzlyak, J.R., A.A. Gitelson, O.B. Chivkunova and V.Y. Rakitin, 1999. Non-destructive Optical Detection of Pigment Changes During Leaf Senescence and Fruit Ripening. *Physiologia Plantarum*, 106: 135-141.
24. Beck, R., 2003, EO-1 User Guide v. 2.3, <http://eo1.usgs.gov/documents.php>
25. Jackson, T.L., D. Chen, M. Cosh, F. Li, M. Anderson, C. Walthall, P. Doriaswamy and E.R. Hunt, 2004. Vegetation Water Content Mapping Using Landsat Data Derived Normalized Difference Water Index for Corn and Soybeans. *Rem. Sens. Environ.*, 92: 475-482.
26. Gates, D.M., 1968. Transpiration and leaf temperature. *Ann. Rev. Plant Physiol.*, 19: 211-238.